Paper Imbibition for Timing of Multi-Step Liquid Handling Protocols on Event-Triggered Centrifugal Microfluidic Lab-on-a-Disc Platforms

David J. Kinahan*[a,b], Sinéad M. Kearney [a,b], Olivier P. Faneuil [a,b,c], Macdara T. Glynn [a,b], Nikolay Dimov [†a,b], and Jens Ducrée[*a,b]

Rotational microfluidic platforms have attracted swiftly growing interest over the last decade due to their suitability for integration and automation of sample preparation and detection. Valving is of pivotal importance on these compact "Lab-on-a-Disc" (LoaD) platforms as all liquids are exposed to the same
10 centrifugal field. A number of valving technologies have been developed to coordinate timing of serial and / or parallel multi-step / multi-liquid assay protocols comprising of laboratory unit operations (LUOs) such as the release, metering and mixing of sample and reagents. So far these valving techniques could be broadly divided into rotationally controlled or externally actuated schemes. Only recently a new, "event-triggered" flow control has been introduced. In this approach, a valve is opened upon arrival of a liquid at
15 a defined destination on the disc; this innovative mechanism for the first time permits the cascading of LUOs independent of the spin rate. In one technology, dissolvable films (DFs) are configured with a pneumatic chamber to offer function akin to an electrical relay. Dissolving one DF, termed the control film (CF), results in the release of liquid at a distal location through a so-called load film (LF). In this paper, a new method for temporal control of these DF-based, event-triggered CFs is introduced. This
20 approach uses a paper strip to transport liquid to the DFs at a certain velocity, thus setting a well-defined interval between subsequent LUOs, e.g. incubation steps. As a proof-of-concept, we present a disc with integrated metering and mixing which can perform a prototypical, 4-fold serial dilution; a common function in bioanalytical protocols. Liquid imbibition along a paper-strip sequentially opens five valves for serial dilution and mixing. To illustrate an unprecedented level of on-disc automation, this is followed
25 by a branched cascade of 17 event-triggered valves (for a total of 22 liquid handling steps) which completes the serial dilution protocol.

1. Introduction

In recent years there has been increased adoption of rotationally controlled LoaD technologies [1-2] for point-of-care / point-of-use
30 applications in fields such as biomedical diagnostics [3], bioprocess monitoring [4] and environmental screening [5-6]. In this LoaD platform the centrifugal force is the main driver for pumping and liquid handling on a cartridge which typically has similar geometry to conventional optical data storage media such as CDs or
35 DVDs. A significant advantage of the centrifugal concept is the ease with which sample can be loaded and processed without need for pressurised fittings or external pumps; providing ruggedness, easy maintenance, ease-of-use, and cost efficiency.
As all liquid residing on a disc is exposed to the same centrifugal
40 field, valving technologies are critical to implement and coordinate a sequence of LUOs [7] including metering, mixing, and reagent release typical of most assay protocols.
Traditional flow control techniques for LoaD platforms could be categorized into externally actuated and rotationally controlled
45 schemes. In the former, a peripheral instrument provides power to ablate sacrificial material or induce a phase-change [8-12], to pressurize [5] or to physically manipulate the disc [13]. This instrument focussed approach expands the number and flexibility of LUOs which can be performed along a single process chain on a
50 cartridge. But this advanced control tends to compromise the innate simplicity of both the instrument and the cartridge at the core of the LoaD system.
The more ubiquitous, rotationally actuated valves are triggered by a change in the disc spin rate which unbalances the equilibrium
55 between centrifugally induced hydrostatic pressure and, for instance, the pressure induced by capillary action or compression of gas pockets. These valves might be categorised into high-pass and low-pass valves. High-pass valves, which are actuated through an increase in spin rate, include capillary burst valves [14-
60 18], centrifugo-pneumatic dissolvable-film (DF) valves[19], burstable foils [20], elastomeric membranes [21] and dead-end pneumatic chambers [22]. Conversely, low-pass valves are actuated through a reduction in the rotational frequency. They are often based on siphons [4, 23-24] where a decrease of the spin rate lets the capillary
65 force prevail the hydrostatic pressure and so liquid can move

radially inbound to prime a siphon channel. As this technology demands a hydrophilic channel which is difficult to stabilize on common polymer surfaces, centrifugo-pneumatic mechanisms based on centrifugally controlled compression of gas have been used to prime even slightly hydrophobic microchannels innate to most polymers [25-26].

The chief drawback of common, rotationally-actuated capillary burst valves is that their operational range is limited by the minimum achievable feature sizes and tolerances associated with their manufacturing techniques. This caps the maximum spin rate available during centrifugal liquid handling and also smears the definition of burst frequencies; both factors thus restrict the number of discrete LUOs which can be automated in a single process. While this limitation has been, to some extent, circumvented through combining low-pass and high-pass valves [4, 23], this strategy can be unreliable and consumes precious disc real-estate.

Lately, a new paradigm in rotational flow control has been introduced. In this event-triggered technique [27], the arrival of liquid at defined locations on the disc prompts the opening of another, distant valve through pneumatic coupling. This technology constitutes an advancement of previously described centrifugo-pneumatic DF valving [19, 28-30] and operates akin to an electrical relay. These valves [27] are composed of a pneumatic chamber sealed by two DFs; called the Load Film (LF) and the Control Film (CF). The pneumatic structure is shaped such that, at typical spin rates, the restrained liquid cannot penetrate into the chamber sufficiently to wet and dissolve either film. However, when the CF is dissolved by an (ancillary) liquid, the restrained liquid enters the pneumatic chamber, wets and dissolves the LF and thus exits through this outlet.

Based on these event-triggered valves a number of LUOs including release of wash reagents, liquid metering and selective liquid routing were demonstrated [27]. In addition, advanced process control such as parallelization and logical operations such as AND-condition triggering [27] was implemented. As a proof-of-concept, these valves were employed for realizing a multi-liquid / multi-step solid-phase RNA extraction protocol on a LoaD platform [27]. These event-triggered valves offer a number of advantages, including operation without peripheral instrumentation and their quasi independence of the spin rate [27]. Nevertheless, a constraint of these valves rests in temporal process control; the interval between subsequent valve actuations depends on the time taken for a liquid to dissolve a DF and the time for the released liquid to be pumped to the CF of the next valve in the cascade. This interval, which is typically of order 120 s, may not suffice for some LUOs such as extended mixing or biological incubation steps.

In this manuscript a new method for actuating event-triggered DF valving is introduced which is based on transporting liquid to the CF of a valve through a low-cost and ubiquitous paper strip [31, 32] integrated on a polymeric disc [33-35]. Combined with the material-specific speed of imbibition, the spacing between the CFs defines the (extended) time span between valve openings. Indeed, imbibition has been used previously to as a valving technology in (non-centrifugal) paper microfluidics [36-38], while the addition of a sucrose solution to paper has been harnessed to modulate the speed of liquid movement [39]. Wicking through paper has also been utilized to trigger electrical / magnetic valves integrated with lateral flow devices [40].

In this paper we first describe the valving concept and the manufacture of the disc. We then present a simplified disc to illustrate the sequential opening of three valves with timing controlled through paper imbibition. Towards application in common assays to determine protein concentrations [41-42], we then demonstrate a four-fold serial dilution (of dyed water) along with the on-disc preparation of calibration controls and the further diluted samples with additional reagents (DI water). This platform orchestrates the opening of a series of five valves by paper imbibition, hence providing sufficient time for mixing LUOs to take place. Furthermore, to underpin the potential of event-triggered valves for large-scale on-disc automation, a further, 17-valves are triggered to run several post-processing steps.

2. Valve Process Control

DF based event-triggered valves [27] are controlled by an ancillary liquid contacting the CF, thereby venting the pneumatic chamber. This way the restrained liquid enters the chamber, wets and dissolves the LF so it can exit through the opened outlet. The time for valve opening is governed by the length of the intervals for the liquid to reach and dissolve the CF, the pneumatic chamber to vent and the time for the LF to be contacted and dissolved.

In the technology introduced in this work, the actuation mechanism of the DF-based event-triggered valves is fundamentally changed to time longer running LUOs. This is implemented through paper imbibition advancing from a reservoir to a sequence of CFs. For DF-based event-triggered valves, a minimum centrifugal field is required to pump the liquid through the pneumatic chamber (typically shaped like a microchannel) to the LF. At given hydraulic diameters and lengths of the microchannels, it then can be assumed that wicking of liquid through paper will be slower than the corresponding microchannel flow. Thus, the speed of the ancillary liquid travelling to the CF is reduced to extend the time span for opening a single valve.

This mechanism is illustrated in Fig. 1. Initially, the DF-based, event-triggered valves will not release liquid from any of the reservoirs, even at high spin rates. Following loading of the ancillary liquid, the paper strip is wetted at one end and the liquid front begins to progress along the paper strip. Upon reaching the CF of a valve, it dissolves, thus venting the pneumatic chamber and permitting the flow of the restrained liquid into the pneumatic chamber. This, in turn, wets and dissolves the LF, consequently opening an exit route through the valve.

It can be inferred from Fig. 1 that as the liquid front progresses further along the paper strip, the CFs for downstream valves will also be wetted and thus opened in sequence. This permits the addition / release of a single liquid on the disc to control a series of valves and so significantly simplify the disc architecture. The sequence of valve opening is defined by the position of the CFs along the paper strip, while the time between valve actuations is defined by the space between the CFs. This interval for the liquid front to advance along the paper strip is also influenced by the grade / thickness of paper and can also be influenced through pre-treatment of the paper strips [39].
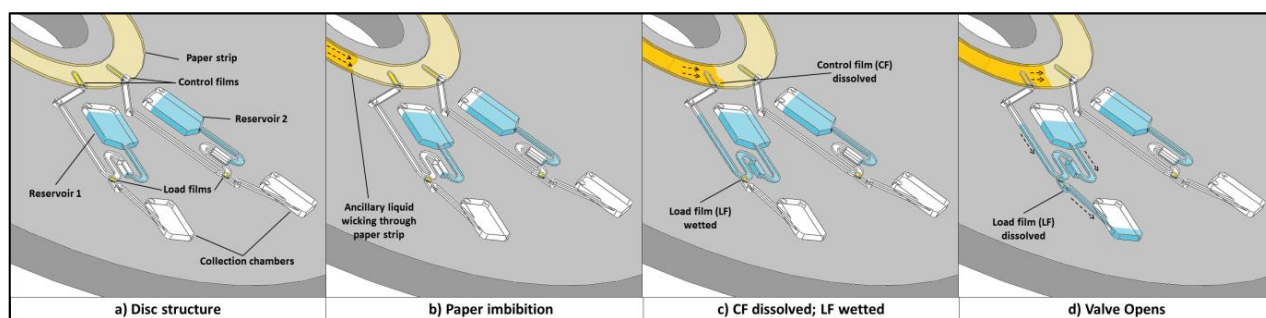
Fig. 1 Paper-based control of valve opening. (a) The event-triggered valves are configured so the control films (CFs) are located along a disc-embedded paper strip. The disc can rotate across a wide range of spin rates while the valves still remain closed. (b) Ancillary liquid is loaded on the disc (or released from an upstream valve) and wets one end of the paper strip to initiate imbibition. (c) The liquid wicking through the paper strip reaches, wets and dissolves the CF. This process vents the trapped gas and allows the sample liquid to enter the valve and wet the LF. (d) The LF dissolves and the liquid is released through the valve. Additional valves, whose CFs are located further down the paper strip, will be triggered with the advancement of the liquid boundary.

3. Materials and Methods

3.1 Disc Assembly, DF Tabs and Experimental Test Stand

The microfluidic discs were assembled from layers of Poly-(methyl methacrylate) (PMMA) and layers of PSA[19,27,43]. A knife-cutter (Graphtec, Yokohama, Japan) created smaller features, such as microchannels, from voids in PSA (86 µm thick). Reservoirs, vents and through-holes were defined by voids defined in the PMMA layers (1.5 mm thick) using a laser cutter (Epilog Zing, USA).

The disc is manufactured using broadly the same layer configurations described previously [27]. In sequence, the outer layer (Layer 1) is manufactured from PMMA and contains loading vents. Layer 2 is cut from PSA and consists of microchannels for pneumatic venting and liquid transport. Note that, for the disc cartridge in the initial study presented in Figure 2, a single layer for PSA was used. For the disc in the serial dilution study, the top-level PSA layer was doubled by rolling two sheets of PSA together before placing it on the knife-cutter. Due to the complexity and density of structures on this disc, it was found that this thicker layer of PSA improved sealing of the disc. For this disc, these identical layers are referred to together as Layer 2 and separately as Layers 2a and 2b.

The large reservoirs for holding liquid are made of voids in the PMMA Layer 3. Layer 4, machined in PSA, acts as a cover supporting the DF tabs. The material cut from this layer also limits the amount of DF material exposed. Note that, during assembly, the paper strip is placed into a reservoir (created by Layer 3) and is adhered to Layer 4 while applying gentle pressure. It should also be noted that the reservoir holding the paper strip is extended through Layers 3-6 at the point where the ancillary liquid contacts the paper strip. This increases the volume available and, as this location is radially farther outwards than the paper strip, ensures the DFs are only wetted through imbibition.
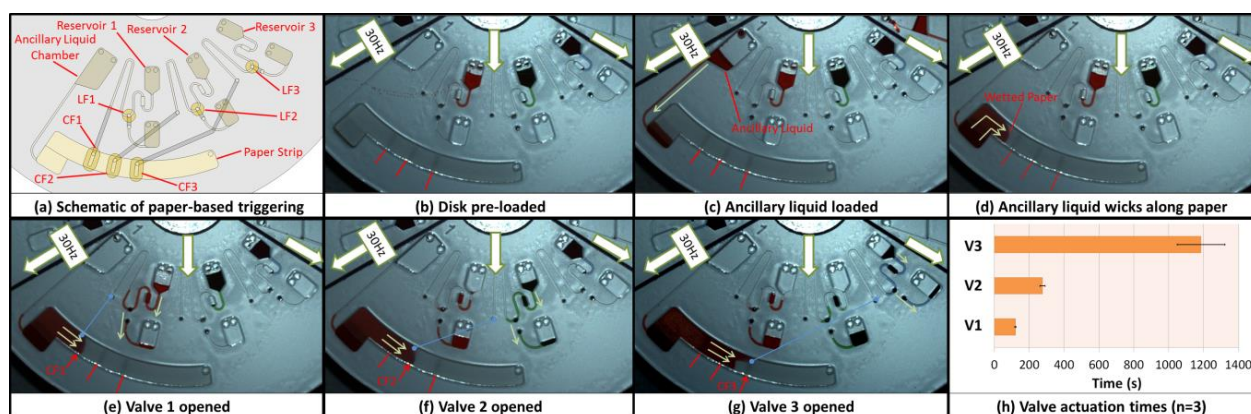

Fig. 2 Serial actuation of valves through paper imbibition. (a) Schematic of this disc architecture. Control films are indicated by CF and the corresponding Load Film by LF. (b) Reservoirs are loaded with pseudo-reagents (dyed water) for visualisation purposes. The valves will not burst at typical spin rates (0 – 60 Hz) until the paper trip is wetted. The locations of the CFs show as dark shadows beneath the paper strip and are also indicated by red arrows. During the experiment the disc rotates at a constant 30 Hz. The direction of centrifugal force is shown by green block arrows. (c) The ancillary liquid is loaded and wets the paper strip. For the duration of the experiment, the spin rate is maintained at a 30 Hz. (d) Liquid wicks along the paper strip (indicated by light green arrows). (e) The liquid front contacts and dissolves CF1, thus venting the pneumatic chamber. As the gas is escapes, Reagent 1 enters the valve, wets LF1 and is released (indicated by light green arrows). The active connecting pneumatic channel is shown by a blue line. (f-g) Valves 2 and 3 are opened using the same mechanism. (h) Burst times for the valves presented here (n = 3). The intervals are measured at the time the CF is observed to be vented (through observation of liquid reaching the LF in the corresponding valve) (see Movie 1 and 2).
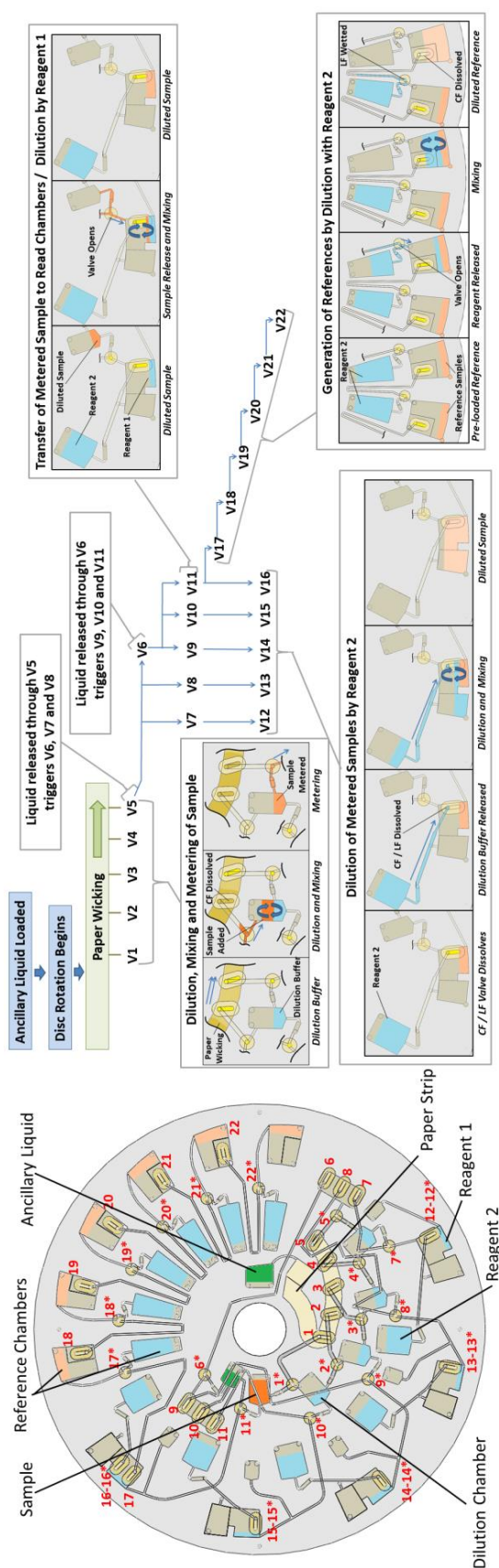
Fig. 3 Schematic of 22-valve disc architecture and flow chart illustrating the control sequence implemented on this disc. The reservoirs, microchannels and pneumatic channels are shown in the disc multi-layer architecture. Due to the size and complexity of the structures, the entire space of the disc (130 mm OD) is occupied. On this disc the valves are numbered in the approximate order at which they trigger. For clarity, in valve components are labelled by number to refer to the CF and starred number refers to the corresponding LF. Co-located CF / LF valves are indicated by both numbers separated by a dash. Liquid heights are indicated where sample and reagents are pre-loaded and the ancillary (paper wetting) liquid has been loaded just prior to starting the experiment. As demonstrated in the flow chart, the experiment is started by loading the ancillary liquid and initiating the disc spin protocol. Firstly, the ancillary liquid wets the paper strip and wicks along it, actuating V1-5 in series. These valves trigger dilution, mixing and metering of the sample. The release of liquid through V5 triggers V7-11 (V9-11 through intermediate actuation of V6) in parallel. V7-11 transfer the diluted sample to a read chamber on the periphery of the disc which has been pre-loaded with Reagent 1. Consequently, the diluted sample mixes with the reagent through swiftly alternating between acceleration and deceleration (30 Hz to 20 Hz). The addition of diluted sample to this chamber in turn triggers V12-16 through wetting and dissolving of the DF located in the read chambers. This prompts the release of Reagent 2 which further dilutes the samples. Additionally, the opening of V11 also triggers actuation of V17, which serially opens V18-22. This generates a series of references where the chambers have been pre-loaded with a known concentration of sample mixed with Reagent 1.

The DF tabs are placed into, and supported by, Layer 5 (PSA). Layer 6 (PMMA) contains through holes to connect microchannels located in the different disc layers, while Layer 7 (PSA) displays the lower-level microchannels for venting and liquid flow. Finally, Layer 8 (PMMA) acts as the floor of these channels. This multi-level architecture isolates microchannels on Layer 2 and Layer 7 and thus permits the channels to cross over.

The paper strip used in the simplified disc was manufactured using a slower wicking paper strip (Whatman CHR Grade 20 (Sigma-Aldrich P/N 3020-917), 170 μm thick, flow rate: 85 mm / 30 min) while a faster grade, (Whatman CHR Grade 1 (Sigma-Aldrich P/N 3001-917), 180 μm thick, flow rate: 130 mm / 30 min) was used for the serial dilution disc. The DFs used in this study are non-adhesive and thus were mounted onto double-sided PSA tabs as described previously [19,27]. The DF (Barnyarns, Rippon, UK), here termed E-film, is a low-cost component based on polyvinyl alcohol which is primarily used for embroidery. This film has been characterised previously [27] and typically dissolve in the presence of DI water in less than 10 s.

A specialised experimental test and development instrument [27, 44, 45], generates images of the disc while in motion. Aside from where otherwise specified, all discs are tested at a spin rate of 30 Hz. The discs are accelerated and slowed down at 12.5 Hz s^{-1}. For the serial-dilution discs, a custom program (written in LabVIEW) varies the rotational frequency between 20 Hz and 30 Hz at set time intervals (10 s). This induces 'shake-mode' mixing [46] by angular acceleration (i.e. the so-called Euler force) and, where valves are present, pneumatically induced mixing [47].

3.2 Measurement of samples on plate-reader

All absorbance measurements were made off-disc using a commercial plate reader (TECAN Infinite® 200 PRO). Initially a series of standard dilutions were generated on-bench to
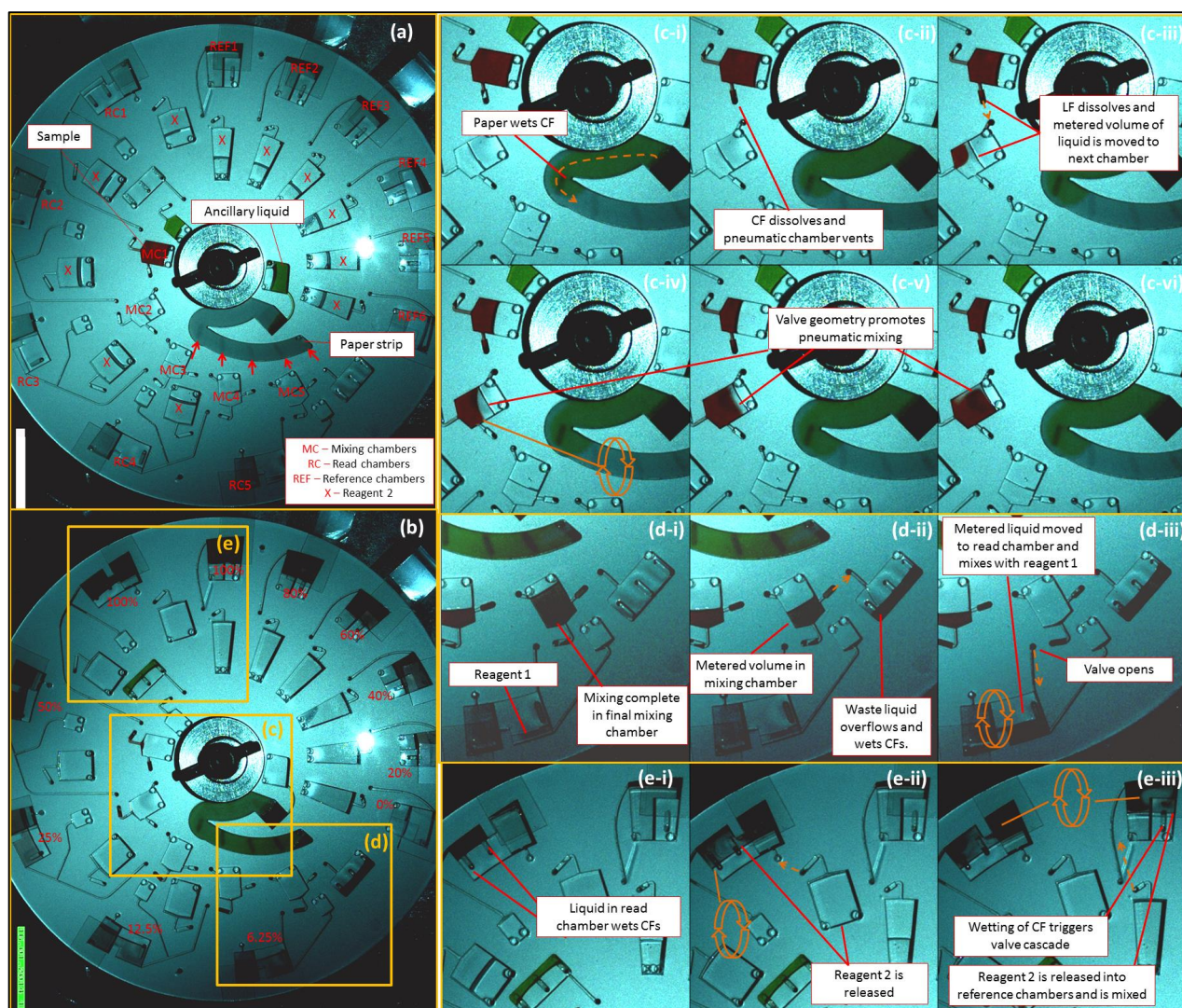
Fig. 4 The serial dilution disc according to the workflow described in Fig. 3. (a) An image of the disc directly after the start of the experiment. Green dyed water wets the base of the paper strip to commence wicking and also as an ancillary liquid to open Valves 9-11. Note that Mixing Chamber (MC) 1 and MCs 2-5 have been loaded with 70 µl of dilute food dye (considered stock, 100% concentration) and 35 µl of DI water, respectively. Each of the read chambers (RCs) has been pre-loaded with 20 µl of DI water and each Diluent Chamber 'X' has been loaded with 160 µl of DI water. Reference RCs 1-6 are pre-loaded with 35 µl of dyed water (of known concentration) and 20 µl of DI water. These concentrations are 100%, 80%, 60%, 40%, 20% and 0%, respectively. (b) Same disc following completion of the liquid handling workflow. Note the different intensity of food dye in the RC and REF chambers (indicating dilution has taken place; nominal dilution in each reservoir is indicated in red text). The overlay boxes indicated the regions shown in the subsequent subfigures (c-i to c-vi) These images show the wetting of CF1 through paper imbibition and the release and transfer of a metered volume of dyed water from MC11 into MC2. (d-i to d-iii) Transfer of liquid from MC5 into the overflow chamber. This leaves a metered volume of liquid present at the base of each MC. (e-i to e-iii) These images show the addition of diluted sample to pre-loaded DI water resulting in the wetting and dissolving of CFs. In all RCs, the dissolution of the co-located CFs / LFs results in the release of the diluent into the RC. In addition, in RC1 (shown) a second CF is dissolved. This triggers the release of diluent into the first Reference Read Chamber (REF) and triggers a cascade of six valve actuations to add diluent to all REFs. Note also in these images that Euler mixing can be observed which was induced by the spin profile (see Movie 3 and 4).

characterise the food dye (Natural Red Food Colour, Dr. Oetker). The peak absorbance of the red dye was recorded at 505 nm. The dye absorbance was measured at a concentration sequence ranging from 0% to 1% of stock food dye diluted in DI water, in 40 µl volumes, in a flat-bottomed, transparent 96-well micro-titre plate (Greiner). From these samples a linear relationship between absorbance and concentration ($r^2 = 0.998$) was established.

In order to determine the concentration of food dye present on-disc, the samples were taken off-disc and pipetted onto the micro-titre plate in duplicate volumes of 40 µl. Absorbance was measured at 505 nm wavelength and the dye concentrations were interpolated using standard curves generated from the reference chambers also present on-disc. Absorbance measurements were not made 'on-disc' as such techniques are widely published [4, 30, 48] and are not the innovation focus of this work.
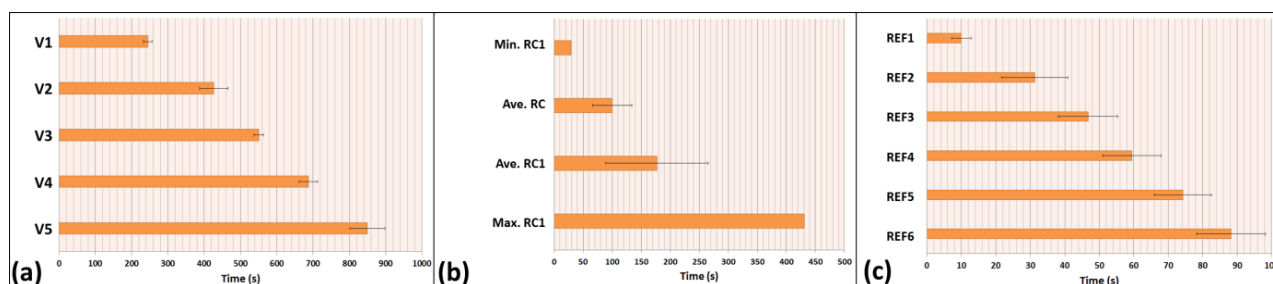
Fig. 5 Timing of Valve Actuation for each stage of the disc. (a) Opening times of valves triggered by paper imbibition measured from the time ancillary liquid wets the paper strip (n = 3) (b) Intervals for addition of Reagent 2 to the read chambers measured relative to the release of liquid through V5. Note that, due to a low pressure head and its radially inward location the intermediate ancillary liquid valve V6 proved to have highly varying and unreliable bust times. In each case, V7 and V8 (triggered directly by opening of V5 and releasing sample into RC4 and 5 respectively), released within 20 s and V12 and V13 followed within another 10 s. However, the addition of sample into RC1-3, and subsequent triggering of the REF chambers relies on actuation of V6. 'Ave. Read Chamber' shows the average time for Reagent 2 to be added into all five read chambers (n = 3). 'Ave Read Chamber 1' shows the average time for Reagent 2 to be added into RC1 (n = 3); 'Min Read Chamber 1' shows the best result while 'Max. Read Chamber 1' shows the worst result. (c) Time of addition of Reagent 2 into each of the Reference chamber relative to the addition of Reagent 2 to RC1 for each disc measured (n = 3).

4. Simplified Valve Actuation Disc

Our first disc cartridge (Fig. 2) implements the sequential release of the three liquids from inner (on-board storage) reservoirs into outer receiving chambers at intervals set by the timing of paper imbibition. To this end three CFs are linearly aligned along the disc-based paper strip. Each CF is pneumatically coupled to a designated LF, so an open CF vents the pneumatic chamber and thus releases the next on-board liquid. Our experiments (n = 3) with the structure in Fig. 2 indeed verified proper sequential release and defined time delays. There was noticeable variation in timing of actuation of the third valve. As this reservoir is depleted (Fig. 2g) the wicking becomes more susceptible to the specific composition of the paper.

5. Serial Dilution Disc

5.1 Serial Dilution Disc Concept and Design

As a pilot study of our novel, imbibition-based flow control scheme towards higher-level process integration, we demonstrate multi-stage serial dilution [41-42] of a starting sample. A protocol is implemented where a sample of dyed water undergoes 4-fold serial dilution (targeting 100%, 50%, 25%, 12.5% and 6.25% final concentrations). These samples are then mixed with two further known liquid volumes (DI water, called Reagent 1 and 2). This representative experiment allows us to demonstrate our multi-step automated liquid handling technology while using volumes consistent with our rapid prototyping technology.

The serial dilution chambers were designed to meter the liquid into a 1:1 ratio ($\log_2$). Chamber geometries were used which resulted in diluted sample volumes of about ~35 µl. After dilution, the sample are first mixed with Reagent 1 (20 µl) and then Reagent 2 (160 µl). Alongside the on-disc dilution of sample, the generation of on-disc references is also shown. The on-disc workflow is shown in Fig. 3.

For the purposes of demonstrating the capabilities of the valves, it is considered that Reagent 2 represents the active agent in a kinetic assay (common in many analyte estimation assays requiring a serial-dilution based standard curve) and thus should be added to both diluted samples and references in as synchronous a manner as possible.

The protocol may be divided into four separate sections:

1. Dilution, mixing and metering of the sample controlled by paper imbibition
2. Transfer of diluted samples to read chambers located on the periphery of the disc and mixing with Reagent 1
3. Addition of Reagent 2 to the read-chambers
4. Addition of Reagent 2 to the reference chambers

5.2 Dilution/Mixing/Metering controlled by paper imbibition

The serial dilution step uses a series of staggered mixing / metering chambers (MCs). Movement of liquid in and out of these MCs during the metering / mixing phase of the workflow is controlled by paper imbibition which is widely independent of spin rate. The mixing chambers (MCs) are divided into two compartments, an upper and lower section. A centrally located valve, dividing the upper from lower sections, can be opened to
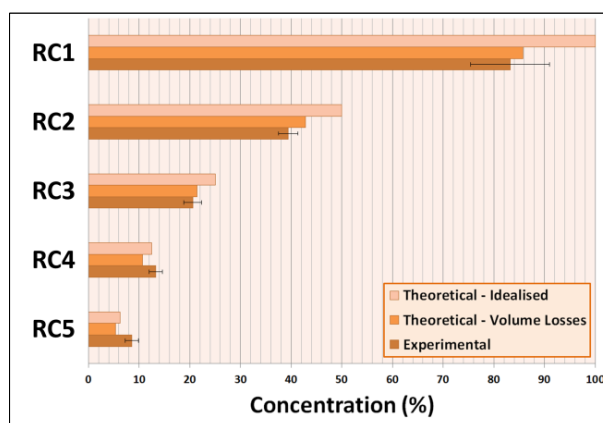

Fig. 6 Concentration of food dye present in each read chamber. 'Theoretical-Idealised' are the theoretical values expected based upon a starting concentration of 100% and $\log_2$ dilution. 'Theoretical – Volume Losses' assumes that there are no fluid losses / dead volume in the upper valve but 5 µl of sample is lost in the lower valve (between the mixing chamber and the read chamber). 'Experimental' are the concentration values estimated based upon the absorption measurements taken from diluted samples and reference samples recovered from the discs (n = 3).

remove liquid from the upper section while the other valve can be opened to remove liquid from the lower section (Figs. 3 and 4). The first MC is fully loaded with sample while the other MCs are half-loaded with dilution buffer. When the first valve (V1) is triggered through paper wetting, ~35 µl of sample is transferred into the second chamber where it mixes with the ~35 µl pre-loaded dilution buffer. The liquids are mixed through a combination of 'shake-mode' Euler mixing [46] and pneumatically induced mixing [47] (a beneficial side-effect of the event-triggered valve geometry). The liquid mixing continues while the paper wicks to the second valve. When this opens, ~35 µl of the now diluted sample is transferred into the next mixing chamber, where it is further diluted. This process repeats until the papers wets and opens V5, whereupon ~35 µl of sample flows into an overflow chamber. At this point each of the five mixing chambers contains ~35 µl of serially diluted sample.

Unlike other valving technologies, the event-triggered valves can function broadly independent of the spin rate. With valve actuation controlled by paper imbibition (thus extending the time between actuations to ~150 s, Fig. 5a), the disc can be subjected to a robust spin profile (alternating the rotational frequency every 10 s between 20 Hz and 30 Hz with acceleration / deceleration at 12.5 Hz s^{-1}) without opening the valves prematurely. This de-coupling of spin rate from valve actuation also enables the afore-mentioned mixing strategies.

The convective mixing is particularly important as it can be seen that, at the high centrifugal field, small density changes can result in stratification of liquids. For example, in Fig. 4c-iv, it can be seen that the red dye settles rapidly to the bottom of the next mixing chamber, displacing the pre-loaded DI water and causing stratification. However, as seen in Fig. 4c-vi, deceleration drives the liquid away from the valve and induces stirring. Similarly, flow patterns seen in Fig. 4e-iii also reveal that Euler mixing also takes place in the read chambers at later stages of the experiment.

5.3 Transfer of diluted samples to read chambers

As described in Figure 3, the actuation of V5 by paper imbibition transfers ~35 µl of dilute sample into an overflow chamber. This results in ~35 µl of sample (at various dilutions) remaining in the bottom of each MC chamber. The movement of this bulk over-flow is used to actuate event-triggered valves [27] which release the diluted sample to move from the mixing chambers to the read chamber located on the periphery of the disc.

Due to the distance between the overflow structure and the MCs on the disc, a staggered approach was used (Fig. 3). The overflow from opening of V5 actuates V6-V8 (Figs. 3 and 4d). V7 and V8 are located at the bases of MC4 and MC5, respectively. However, opening V6 releases an ancillary liquid located in a reservoir which is closer to MC1-MC3. Thus, opening V6 releases this ancillary liquid which, in turn, opens V9-V11 to transfer liquid from MC1-3 to their respective read chambers. The dilute samples then flow into the RC chamber where they can mix with pre-loaded Reagent 1 (20 µl).

However, it was found that in most cases Valve 6 did not trigger within the expected time-frame; in one case it took over 7 minutes (Fig. 5b). This is primarily a result of poor manufac-turing fidelity, the radially inward location of the ancillary liquid and the small fluid volume (leading to a small hydrostatic pressure head) combining with slightly hydrophobic PSA and

PMMA to stop this particular valve functioning promptly. Nevertheless, in the cases where this valve opened within an expected time frame all diluted samples were added to their respective read chambers within a ~30 s window.

5.4 Dilution of Sample in Read Chambers

The addition of dilute sample (~35 µl) to the pre-loaded Reagent 1 (20 µl) in the read chambers increases the liquid height within the chamber. This brings the liquid in contact with the DFs located within the chambers. RC1 contains two DFs (V16 and V17) located at a single height while the other RCs contain one DF. Valves 12-16 are co-located CF / LF event-triggered valves [27] (where a single DF acts as both the CF and LF). The triggering liquid wets the DF from the 'underside' which releases the restrained liquid to mix with the ancillary liquid via Euler mixing induced by the ongoing rapid acceleration and deceleration of the disc (Figs. 3 and 4e). In every case, the addition of Reagent 2 to the read chamber occurs in < 10 s after the DF film is wetted.

5.5 Reference Chambers

Alongside the sample dilution, a series of reactions of known concentrations (to generate a reference curve) are also generated on-disc. This is particularly useful for kinetic assays as, for valid measurements, kinetic reagents (assumed here, for this case, to be Reagent 2) must be added to both diluted samples and reference samples within a small time window.

A series of reference chambers (REF1-6) are pre-loaded with known concentrations of sample (35 µl of 100%, 80%, 60%, 40%, 20% and 0% concentration). 20 µl of Reagent 1 is then loaded into chambers REF1-6, respectively.

Upon addition of sample to RC1 (as described above), a valve is actuated (wetting of CF17) and cascades the release of Valves 17-22. This releases 160 µl of Reagent 2 into each reference chamber to mix with the pre-loaded sample / Reagent 1 mixture (Figs. 3 and 4e).

The actuation times for V17-22 (REF1-6), relative to the addition of sample to RC1, are shown in Fig. 5c. It can be seen that these valves triggered rapidly (~15 s per valve); all six valves were actuated in 71 s.

5.6 Serial Dilution Results

Figure 6 shows the absorbance measured experimentally from the sample dilution chambers (RC1-5). These values are compared to two theoretical models. In the first instance, it is assumed that the chambers function perfectly by design (mixing the liquids until they are fully uniform and then metering them into precisely 35 µl aliquots, which are transported without loss / dead volume about the disc). Nevertheless, as can be seen the values measured from RC1, which is the pre-loaded 100% stock, showed lower concentration than expected. A second model is also shown which assumes good mixing but, while 35 µl of liquid is moved into the next mixing chamber, only 30 µl arrived at the read chambers due to losses. This model proves to be a better model of the system performance for the first three read chambers.

From the experimental data, two final chambers (RC4 and RC5) were found to have higher concentrations than would be expected from either of the theoretical models. In fact, the ratio of each dilution to the next is 2.1, 1.9, 1.5, 1.6, meaning the first chamber dilutes the sample more than expected by design while the

subsequent chambers dilute it less than by design.

This effect is most likely a result of losses to dead volumes in the valves and microchannels (as observed during experiments) and / or variation in system performance due to the differing radial positions of the mixing chambers (i.e. different flow properties due to the different local centrifugal force).

While these issues bear further investigation, it should be noted that, from disc to disc / chamber to chamber (Fig. 6), the variation in the dilution ratio was quite small. Therefore, it is entirely feasible that through system characterisation, iterative design and better manufacture a highly automated and repeatable system might be created based on this technology.

6. Conclusions and Outlook

A severe limitation of recently introduced, event-triggered centrifugal flow control is the dependence of valve actuation on the dissolution time of a DF and the transfer time of the liquid involved. In this work a new concept for valve actuation is introduced which employs the relatively slow and well-defined speed of imbibition of common paper material to clock as well as extend the interval between successive valve openings. This new time control function now enables common LUOs such as incubation with reagents or kinetic reactions which require longer or tightly-controlled process times.

Along with increasing the scope of temporal process control, this technology offers further benefits. The ability to place CFs at known spaces along a paper strip permits an extended sequence of process steps to be initiated through the movement of a single liquid element. This has particular advantages for complex processes, as the use of a single paper strip to trigger multiple valves can simplify disc architectures relative to the use of conventional, DF-based event-triggered valves. However, a challenge of this approach is the strict dependency between valve actuations is lost; should a CF not be wetted / dissolve fully, but a downstream CF is, the valve actuation sequence will be disarrayed.

Due to their independence of the spin rate, event-triggered valves (actuated by both paper imbibition and bulk flow) enable LUOs which are governed by the spin profile. In this case, it enabled aggressive Euler and pneumatic mixing through the use of a 'shake-mode' spin profile. In addition, aside from a single valve which was affected by manufacturing issues, it was found that both the paper imbibition and bulk flow triggered valves actuated within reliable time frames. This is very important both, to permit sufficient time for mixing and to enable kinetic assays on this platform. In fact, it may be inferred that, with more robust design and better manufacturing techniques, kinetic reagents can be delivered to all eleven read chambers in less than 100 s.

Beyond timing of DF-based event-triggered flow control, paper wicking can endow further the capabilities of the LoaD platform. For example, the already established modulation of the speed of paper imbibition via the centrifugal force to modulate [33] may leverage novel schemes for high- and low-pass valving.

In conclusion, we demonstrated paper-triggered DF valves can be combined with the previously introduced, event-triggered valves to coordinate the timing of a complex series of LUOs on a disc independent of the spin rate. In this work, an unprecedented level of automation has been introduced through the implementation, in parallel and in series, of 22 discrete liquid handling steps.

Footnotes

[*] Corresponding Authors: David Kinahan: david.kinahan@dcu.ie; Jens Ducrée: jens.ducree@dcu.ie

[a] Biomedical Diagnostics Institute, National Centre of Sensor Research, Dublin City University, Glasnevin, Dublin 9, Ireland

[b] School of Physical Sciences, Dublin City University, Glasnevin, Dublin 9, Ireland

[c] Telecom Physique Strasbourg; Université de Strasbourg; Strasbourg; France

[†] Current Affiliation: Dept. of Biochemical Engineering, University College London, United Kingdom

References

1. J. Ducrée, S. Haeberle, S. Lutz, S. Pausch, F. von Stetten, R. Zengerle, *J Micromech Microeng*, 2007, 17 :S103-S115 (DOI: 10.1088/0960-1317/17/7/S07).

2. M. Madou, J. Zoval, G. Jia, H. Kido, J. Kim, N. Kim, *Annu. Rev. Biomed. Eng.*, 2007, 8 : 601-628 (DOI: 10.1146/annurev.bioeng.8.061505.095758).

3. R. Gorkin, J. Park, J. Siegrist, M. Amasia, B.S. Lee *et al.*, *Lab Chip*, 2010, 10(14): 1758-1773 (DOI: 10.1039/B924109D).

4. C.E. Nwankire, G. Donohoe, X. Zhang, J. Siegrist, M. Somers *et al.*, *Analytica Chimica Acta* 2013, 781: 54-62 (DOI: 10.1007/s10404-013-1266-x).

5. M.C.R. Kong, E.D. Salin, *Anal. Chem.* 2012 84(22): 10038–10043 (DOI: 10.1021/ac302507t).

6. H. Hwang, Y. Kim, J. Cho, J. Lee, M.S. Choi *et al.* (2013) *Anal. Chem.* 85(5): 2954-2960 (DOI: 10.1021/ac3036734).

7. J.W. Hurst, J.W. Mortimer, Laboratory Robotics, a Guide to Planning, Programming and Applications *VCH Publishers Inc*, 1987.

8. P. Zucchelli, B. van de Vyver, Patent document WO200405024, 2004.

9. J.L. García-Cordero, D. Kurzbuch, F. Benito-Lopez, D. Diamond, L.P. Lee *et al.*, *Lab Chip*, 2010, 10(20): 2680-2687 (DOI: 10.1039/c004980h).

10. B.S. Lee, Y.U. Lee, H.S. Kim, T.H. Kim, J. Park *et al.*, *Lab Chip*, 2011, 11(1): 70-78 (DOI: 10.1039/c0lc00205d)

11. K. Abi-Samra, R. Hanson, M. Madou, R. Gorkin, *Lab Chip*, 2011, 11(4): 723-726 (DOI: 10.1039/c0lc00160k).

12. W. Al-Faqheri, F. Ibrahim, T. Hwai, G. Thio, J. Moebius *et al.*, *PLOS ONE* 2013, **8**(3): e58523 (DOI: 10.1371/journal.pone.0058523).

13. T. Kawai, N. Naruishi, H. Nagai, Y. Tanaka, Y. Hagihara *et al.*, *Anal. Chem.*, 2013, **85**(14): 6587–6592 (DOI: 10.1021/ac400667e)

14. J. Chen, P. Huang, M. Lin *Microfluidics Nanofluidics*, 2008, **4**(5): 427-437 (DOI: 10.1007/s10404-007-0196-x).

15. J.L. Moore, A. McCuiston, I. Mittendorf, R. Ottway, R.D. Johnson, *Microfluidics Nanofluidics*, 2011, 10(4): 877-888 (DOI: 10.1007/s10404-010-0721-1).

16 T. Hwai, G. Thio, S. Soroori, F. Ibrahim, W. Al-Faqheri *et al.*, *Med Biol Eng Comput*, 2013, 51(5): 525-535 (DOI: 10.1007/s11517-012-1020-7).

17. T. Li, L. Zhang, K.M. Leung, J. Yang, *J Micromech. Microeng*, 2010, 20 (10): 105024 (DOI:10.1088/0960-1317/20/10/105024).

18. S. Haeberle, T. Brenner, R. Zengerle, J. Ducrée *Lab Chip*, 2006, 6(6): 776-781 (DOI: 10.1039/B604145K).

19. R. Gorkin, C.E. Nwankire, J. Gaughran, X. Zhang, G. Donohoe *et al.*, *Lab Chip*, 2012, 12(16): 2894-2902 (DOI: 10.1039/C2LC20973J).

20. T. van Oordt, Y. Barb, J. Smetana, R. Zengerle, F. von Stetten, *Lab Chip* 2013, 13 (15): 2888-2892 (DOI: 10.1039/C3LC50404B).

21. H. Hwang, H.H. Kim, Y.K. Cho, *Lab Chip*, 2011, 11 (8): 1434-1436 (DOI: 10.1039/C0LC00658K).

22. D. Mark, P. Weber, S. Lutz, M. Focke, R. Zengerle *et al*., *Microfluidics Nanofluidics* 2011, 10(6): 1279-1288 (DOI: 10.1007/s10404-010-0759-0).

23. J. Siegrist, R. Gorkin, L. Clime, E. Roy, R. Peytavi *et al*., *Microfluidics Nanofluidics* 2009, **9**(1): 55-63 (DOI: 10.1007/s10404-009-0523-5).

24. M. Kitsara, C.E. Nwankire, L. Walsh, G. Hughes, M. Somers *et al*., *Microfluidics Nanofluidics*, 2013, *(*DOI: 10.1007/s10404-013-1266-x)

25. R. Gorkin, C. Liviu, M. Madou, H. Kido, *Microfluidics Nanofluidics* 2010, **9**(2): 541-549 (DOI: 10.1007/s10404-010-0571-x).

26. N. Godino, R. Gorkin, A.V. Linares, R. Burger, J. Ducrée *Lab Chip*, 2013, **13**(4): 685-694 (DOI: 10.1039/C2LC40722A).

27. D.J. Kinahan, S.M. Kearney, N. Dimov, M.T. Glynn and J. Ducrée *Lab Chip*, 2014, (DOI: 10.1039/C4LC00380B).

28. C.E. Nwankire, D.S.S Chan, J. Gaughran, R. Gorkin *et al*., *Sensors* 2013, **13**(9): 11336-11349 (DOI:10.3390/s130911336).

29. C.E. Nwankire, M. Czugala, R. Burger, K.J. Fraser, T. M. O'Connell, *et al*., *Biosensors and Bioelectronics*, 2014, **56** : 352**–**358 (DOI: 10.1016/j.bios.2014.01.031).

30. N. Dimov, J. Gaughran, D. McAuley, D. Boyle, D.J. Kinahan *et al*. in *proceedings of Micro Electro Mechanical Systems (MEMS 2014)*, San Francisco, USA pp 260-263

31. A.W. Martinez, S. T. Phillips, G.M. Whitesides, and E. Carrilho. *Anal*. *Chem*. **82**, no. 1 (2009): 3-10. (DOI**:** 10.1021/ac9013989).

32. D. Cate, W Dungchai, J. Cunningham, J. Volckens, and C. Henry. *Lab Chip* 2013,**13**: 2397-2404 (DOI**:** 10.1039/C3LC50072A)

33. E. Vereshchagina, K. Bourke, L. Meehan, C. Dixit, D. Mc Glade *et al*. in *Proceedings of the 26th IEEE International Conference on Micro Electro Mechanical Systems (MEMS 2013*), Taipei, Taiwan, pp 1049-1052. (DOI: 10.1109/MEMSYS.2013.6474429).

34. N. Godino, E. Vereshchagina, R. Gorkin III, and J. Ducrée. *Microfluidics and Nanofluidics* , 16(5):895–905, 2014, DOI:10.1007/s10404-013-1283-9.

35. TH Kim, J. Park, CJ Kim, and YK Cho. *Anal*. *Chem*., 2014, *86* (8), pp 3841–3848 (DOI: 10.1021/ac403971h).

36 S. Jahanshahi-Anbuhi, A. Henry, V. Leung, C. Sicard, K. Pennings *et al*., *Lab Chip* 2014, 14: 229-236. (DOI: 10.1039/C3LC50762A).

37. J. Houghtaling, T. Liang, G. Thiessen, and E. Fu. Anal. Chem. 2013, 85: 11201-11204. (DOI: 10.1021/ac4022677).

38. GE Fridley, HQ Le, E Fu, and P Yager. " *Lab Chip*, 2012, 12: 4321-4327. (DOI: 10.1039/C2LC40785J).

39. B. Lutz, T. Liang, E. Fu, S Ramachandran, P. Kauffman *et al*., Lab Chip, 2013, 13:2840-7. (DOI: 10.1039/c3lc50178g).

40. X. Li, P. Zwanenburg and X. Liu., *Lab Chip*, 2013, **13**, 2609-2614 (DOI: 10.1039/C3LC00006K).

41. M. M . Bradford, *Analytical Biochemistry* 72, no. 1 (1976): 248-254.

42. O.H. Lowry, NJ. Rosebrough, A.L. Farr, and R.J. Randall. *J*. *Biol*. *Chem*. 193, no. 1 (1951): 265-275.

43. D.A. Bartholomeusz, R.W. Boutté, J. D. Andrade, Microelectromechanical Systems 2005, 14(6): 1364-1374 (DOI: 10.1109/JMEMS.2005.859087).

44. M. Grumann, T. Brenner, C. Beer, R. Zengerle, J. Ducrée, Review of Scientific Instruments, 2005, 76(2):025101 (DOI: 10.1063/1.1834703).

45. D. Kirby, J. Siegrist, G. Kijanka, L. Zavattoni, O. Sheils *et al*., *Microfluidics Nanofluidics*, 2012, 13(6): 899-908 (DOI: 10.1007/s10404-012-1007-6).

46. Grumman, M, *et al*., Lab Chip, 2005, 5: 560-565. (DOI: 10.1039/B418253G).

47. Z. Noroozi, H. Kido, M. Micic, H. Pan, C. Bartolome et al, *Review of Scientific Instruments*, 2009, 80 (7) 075102 (DOI: 10.1063/1.3169508).

48. M. Czugala, D. Maher, F. Collins, R. Burger, F. Hopfgartner *et al*., *RSC Advances, 2013*, 3: 15928-15938. (DOI: 10.1039/C3RA42975J).